Iranian Journal of Basic Medical Sciences
ijbms.mums.ac.ir

Radiosensitization effects of $BaTiO_3$ and gold nanoparticles in proton therapy of pancreatic tumors: A Monte Carlo study

Elham Mansouri [1], Parinaz Mehnati [1, 2*]

[1] Medical Radiation Sciences Research Center, Tabriz University of Medical Sciences, Tabriz, Iran.
[2] Medical Physics Department, Faculty of Medicine, Tabriz University of Medical Sciences, Tabriz, Iran

ARTICLE INFO

Article type:
Original

Article history:
Received: Apr 11, 2026
Accepted: Aug 5, 2026

Keywords:
Barium titanate
MCNP6
Pancreatic tumor
Proton therapy
Radiosensitization

ABSTRACT

Objective(s): This study investigates the potential of barium titanate ($BaTiO_3$) nanoparticles to enhance the therapeutic efficacy of proton therapy for pancreatic tumors in comparison to gold nanoparticles through both macroscopic and microscopic simulations.

Materials and Methods: Using the MCNP6.1 Monte Carlo code, we modeled a 3cm pancreatic tumor in the head of the pancreas loaded with clusters of $BaTiO_3$ and gold nanoparticles using a lattice model. Proton beam (SOBP, 135 MeV) interactions were simulated to evaluate the dose enhancement factor (DEF) within the tumor, the non-tumor pancreas, and Organs At Risks (OARs). Additionally, microscopic dosimetry was conducted to study the dose deposition in the vicinity of the clusters containing nanoparticles.

Results: The gold nanoparticles present DEF of 1.21 and $BaTiO_3$ nanoparticles present DEF of 1.14 in the tumor site. The OARs remained mainly unaffected. Also, on a microscopic scale, DEF values of 1.7-1.83 in the presence of gold nanoparticles and 1.42-1.51 in the presence of $BaTiO_3$ nanoparticles were calculated. The microscopic DEFs were more than the macroscopic DEF.

Conclusion: Both gold and $BaTiO_3$ nanoparticles enhanced proton dose deposition, with gold nanoparticles producing greater macroscopic and microscopic DEFs. The results also show that microscopic dose enhancement exceeds macroscopic dose enhancement, confirming that most proton-induced dose enhancement occurs in the close vicinity of nanoparticles. Because this study is based on Monte Carlo simulations with a uniform nanoparticle distribution and without biological modeling, further experimental studies are needed to validate these findings.

▶ Please cite this article as:
Mansouri E, Mehnati P. Radiosensitization effects of $BaTiO_3$ and gold nanoparticles in proton therapy of pancreatic tumors: A Monte Carlo study. Iran J Basic Med Sci 2026; 29:

Corrected Proof

Introduction

Pancreatic cancer remains one of the most lethal malignancies due to its aggressive nature, late diagnosis, and complex anatomical location near critical organs (1). Proton therapy has emerged as an effective treatment modality, offering superior dose conformity and sparing of healthy organs compared to conventional photon therapy, primarily due to the Bragg peak phenomenon that allows protons to deposit most of their energy at a specific depth (2). However, achieving sufficient tumor control in pancreatic cancer remains challenging because of its radioresistance and the need to limit doses to surrounding organs at risk (OARs). Nanoparticles, defined as particles with dimensions less than 100 nm, possess a high surface-to-volume (S/V) ratio and exhibit effective cellular uptake (3). Various nanoparticles, including metallic and metal oxide nanoparticles (such as several ceramic oxides), have been investigated for their radiosensitization potential in proton therapy (3-6). Metallic nanoparticles such as gold (Au), owing to their high atomic number and density, facilitate increased local energy deposition within tumors (7). Most radiosensitization studies have focused on high-Z metals like gold. However, alternative materials to metal nanoparticles have been less studied with respect to cost and biocompatibility. $BaTiO_3$ nanoparticles have high potential for use in targeted cancer therapy (8). Studying the radiosensitization potential of $BaTiO_3$ nanoparticles, an inorganic ceramic compound known for its ferroelectric and biocompatible properties, could be beneficial in introducing an alternative to gold. Barium (Z=56) contributes significantly to ionization events through Coulomb interactions with protons.

Monte Carlo modeling enables the optimization of nanoparticle type, size, and proton beam parameters before experimental and clinical studies, facilitating safer and more effective treatment planning. Monte Carlo codes such as MCNP6 provide detailed modeling of particle transport and interactions in heterogeneous geometries, offering insight into dose distributions at both macroscopic and microscopic scales (9). Actually, MCNP6 has merged the legacy code of two previous versions, MCNP5 and MCNPX, incorporating high-energy particles and light ions. Unlike MCNPX, MCNP6.1 can transport electrons below 1 keV.

***Corresponding author:** Parinaz Mehnati. Medical Radiation Sciences Research Center, Tabriz University of Medical Sciences, Tabriz, Iran. Email: Parinazmehnati8@gmail.com, mehnatip@tbzmed.ac.ir

© 2026. This work is openly licensed via CC BY 4.0.
This is an Open Access article distributed under the terms of the Creative Commons Attribution License (https://creativecommons.org/licenses), which permits unrestricted use, distribution, and reproduction in any medium, provided the original work is properly cited.

MCNP6 has extended the minimum energy cutoff for photon transport down to 1 eV. These simulations are indispensable for studying nanoscale phenomena such as dose enhancement by nanoparticles, especially when experimental methods are limited by resolution or ethical constraints.

In this study, we performed a detailed MCNP6.1 simulation of a pancreas tumor loaded with gold and $BaTiO_3$ nanoparticles and irradiated it with a monoenergetic therapeutic proton beam. The model geometry includes surrounding OARs. Also, in this study, by comparing absorbed doses with and without nanoparticle inclusion, the macroscopic and microscopic DEF is calculated to evaluate the potential of $BaTiO_3$ nanoparticles for enhancing the therapeutic ratio in proton therapy for pancreatic cancer compared to gold nanoparticles.

The results of this study, by providing a detailed analysis of proton interactions with $BaTiO_3$ and comparing them with those of gold, establish a solid foundation for the design and optimization of radiosensitizers, paving the way for future studies ranging from clinical simulations to biological evaluations. These findings support further preclinical validation and eventual clinical translation, offering a pathway toward more effective, personalized proton therapy for pancreatic cancer.

Materials and Methods

Simulation platform

All simulations were conducted using MCNP6.1 (Monte Carlo N-Particle Transport Code, Los Alamos National Laboratory), a widely validated Monte Carlo code capable of simulating detailed particle transport (10). Its capacity to handle complex geometries and dose tallies makes it highly suitable for studying dose enhancement factors (DEF) induced by nanoparticles (NPs) in proton therapy. In MCNP6, the Coulomb diffusion and the energy straggling of protons, as well as elastic and inelastic scatterings, were taken into account.

Geometry and organ definition

Simplified MCNP6 surface and cell cards were used to approximate the pancreas and adjacent organs at risk (OARs): liver, duodenum, and stomach (Figure 1). These structures were placed based on anatomical proximity, with spatial separation approximating real human anatomy to evaluate dose distributions (pancreas (length: 12 cm, head diameter: 3 cm, width:2.5); liver (length:15 cm); stomach (diameter 6 cm, length:10 cm and width 4 cm); kidney (11 cm (length), 6 cm (width), and 4 cm (depth); duodenum (length:25 cm, diameter:4.5 cm). A grade 3 pancreatic tumor (~3.5 cm diameter) was embedded within the head of the pancreas. The density of the non-tumor pancreas was 1.04 g/cm³. Also, the density of the OARs is: (liver:1.06 g/cm³, stomach: 1.02 g/cm³, duodenum:1.02 g/cm³, kidney:1.05 g/cm³)(11). The simulated organ characteristics are presented in Table 1.

Table 1. Simulated organ characteristics and anatomical parameters used in the MCNP6 model

Organ	Density (g/cm³)	Dimensions
Pancreas	1.04	12×3×2.5 (cm)
Liver	1.06	15×12×10 (cm)
Stomach	1.02	10×6×4 (cm)
Duodenum	1.02	3.5×25 (cm)
Kidney	1.05	11×6×4 (cm)

Proton beam and SOBP configuration

A 135 MeV monoenergetic proton beam source was modeled as a monodirectional disk-shaped source (0.5 cm radius) located above the pancreas tumor center. It is assumed that the proton current used for therapy is 1 μA, and the dose required to kill cancer cells is 35 Gy. A Spread-Out Bragg Peak (SOBP) was implemented by convoluting monoenergetic proton energies to ensure a uniform dose across the entire tumor volume. Nuclear interaction data for protons and secondary particles were taken from the TENDL-2021 library, which provides evaluated cross sections for proton-induced reactions up to 200 MeV.

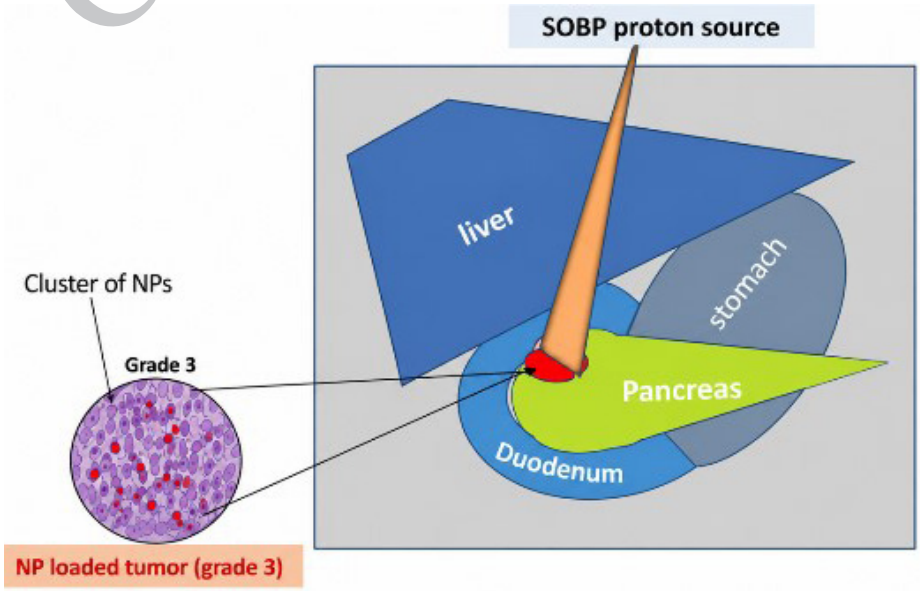

Figure 1. Geometry of simulation
A pancreatic tumor (3 cm) located in the head of the pancreas is exposed to a 135 MeV SOBP proton source (35Gy). Also, organs at risk are presented.
SOBP: Spread-out bragg peak

Corrected Proof

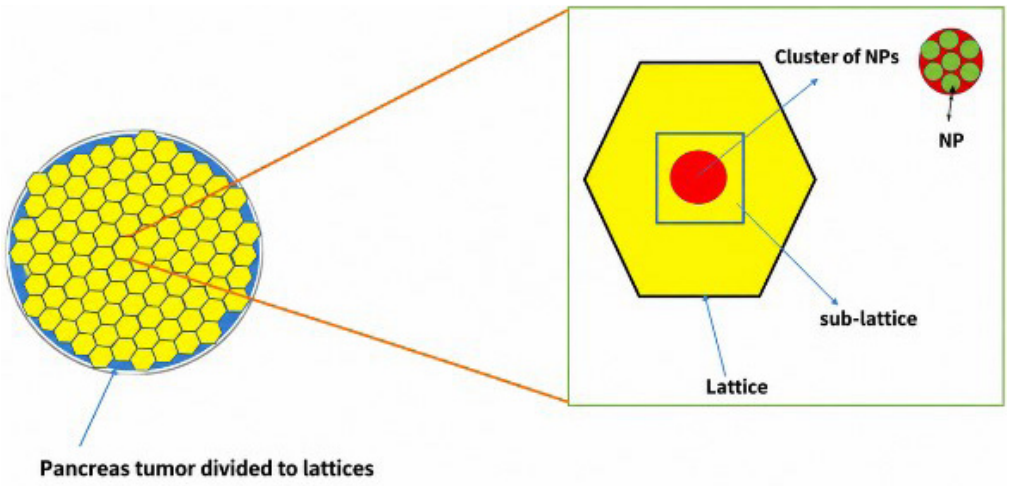

Figure 2. Macroscopic and microscopic view of a pancreatic tumor divided into lattices (10 μm^3)
To provide a 10 mg/g concentration of nanoparticles in the tumor, each lattice contains a cluster of gold or barium titanate nanoparticles with 540 gold nanoparticles and 520 barium titanate nanoparticles in each cluster. Also, the dose deposition was calculated in a cubic (1.25 μm^3) sub-lattice located in each lattice, which contains the cluster.
NP: Nanoparticle

Atomic and electromagnetic data (stopping powers, scattering, ionization) were obtained from MCPLIB and validated against NIST PSTAR data for proton energy loss in tissue and nanoparticle material.

Nanoparticle modeling

Two groups of nanoparticles—gold (Au: Z=79, ρ = 19.3 g/cm^3) and barium titanate ($BaTiO_3$: Ba (Z=56), Ti (Z=22), O (Z=8), ρ = 6.02 g/cm^3)—were modeled using a nanolattice distribution within the tumor. Nanoparticles were placed in a structured array to simulate local clustering (inter-particle spacing ~15 nm). Spherical clusters with a nominal diameter of 200 nm contained nanoparticles of 10 nm.

In Monte Carlo radiation transport codes, a lattice is a regularly repeating array of identical or parametrized unit cells used to model complex and periodic geometries efficiently. In this study, a lattice structure with a hexagonal 3D array of spherical nanoparticle clusters was placed in the center of the tumor to interact with the microscopic beam transporting through the tumor. A nanoparticle cluster is a localized aggregation of multiple nanoparticles that are spatially grouped within a small region rather than being uniformly dispersed.

Based on the literature review, the concentration of nanoparticles was set to 10mg/g of the tumor (12, 13). The lattice model enabled us to provide a homogeneous distribution of nanoparticles, because the concentration of nanoparticles in the tumor is 10mg/g tumor tissue. To provide the nanoparticle concentration of 10 mg/g of tumor tissue, the tumor volume was divided into three-dimensional lattices (10μm^3). Each lattice contains a 200 nm cluster of nanoparticles, with 540 gold nanoparticles and 520 barium titanate nanoparticles in each cluster. Also, to score dose deposition in the vicinity of the nanoparticle clusters, a cubic (1.25 μm^3) sub-lattice was placed in each lattice (Figure 2). In this study, a lattice structure with a hexagonal 3D array of spherical nanoparticle cluster was placed in the center of the tumor to interact with the microscopic beam transporting through the tumor. A nanoparticle cluster is a localized aggregation of multiple nanoparticles that are spatially grouped within a small region rather than being uniformly dispersed.

In this study, the main goal was to compare the radiosensitization properties of barium titanate and gold nanoparticles in proton therapy. Although the heterogeneous distribution is more realistic, the homogeneous distribution was simpler and achieved the objectives of this research.

DVH and source distance analysis

Dose-volume histograms (DVH) were extracted from mesh tally data using post-processing scripts. To achieve tumor coverage, source-to-tumor distances of 7.5–15 cm were simulated. The goal was to find the optimal tumor-source distance to achieve maximum V90% ~100% (volume receiving ≥90% of the prescribed dose) within the tumor.

Dose tally and DEF calculation

Dose deposition was tallied using F6 (MeV/g) in MCNP6 across the tumor, non-tumor pancreas, and OARs. The deposited energy (MeV/g) was converted to absorbed dose (Gy) by multiplying the energy by $1.6*10^{-10}$).

The DEF was calculated using the equation below:

DEF=(absorbed dose of radiation in the presence of NPs/absorbed dose of radiation in the absence of NPs)

Therefore, the dose enhancement factor shows the efficacy of nanoparticles in dose absorption with radiation. The macroscopic dose enhancement was calculated in the tumor. Also, the microscopic dose deposition was calculated in lattices and cubic (1.25 μm^3) sub-lattices which are located in the center of each lattice (Figure 2).

Each simulation was run with ≥10^8 proton histories, ensuring statistical uncertainties ≤2% in all regions.

Results

To achieve optimum tumor coverage, source-to-tumor distances up to 15 cm were considered. The goal was to achieve V90% ~100% (volume receiving ≥90% of the prescribed dose) within the tumor and find the suitable distance. Figure 3 shows that at a 13.5 cm source-to-tumor distance, 98.78% of the tumor receives≥90% of the prescribed dose. The homogeneity index (HI) is about 100%, and the conformity index (CI) is 98.76%. The D_{Max} is 34.89

Corrected Proof

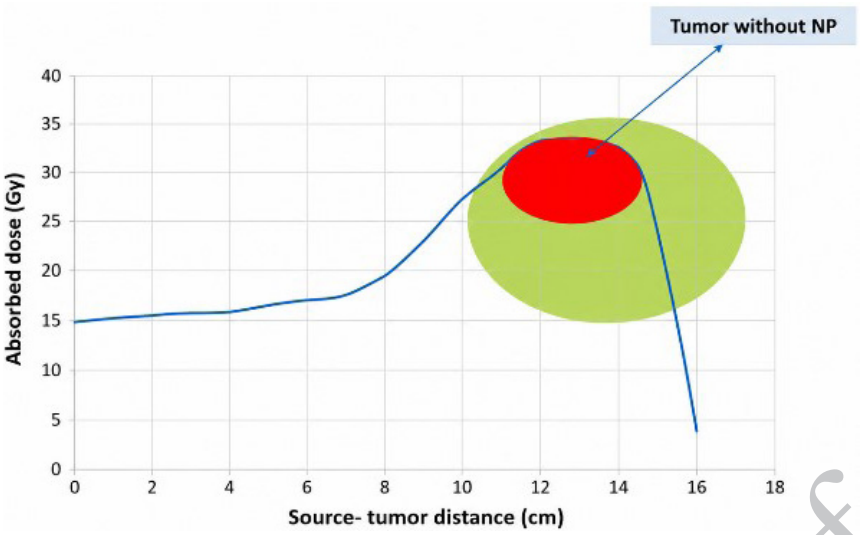

Figure 3. In proton SOBP source-tumor distance of 13.5 cm, 98.87% of the tumor volume receives more than 90% of the treatment dose
SOBP: Spread-out bragg peak

Gy, and Dmean is 34.45 Gy. Thus, we used the source-to-tumor distance of 13.5 cm to study the dose enhancement effect of Au and $BaTiO_3$ nanoparticles.

Figures 4 a and b show the results of DEF values in the tumor, non-tumor pancreas, and organs at risk irradiated by a proton beam with an energy of 135 MeV SOBP when the pancreas is loaded with $BaTiO_3$ or gold nanoparticles. As the results show, both nanoparticles show a measurable increase in absorbed dose within the tumor when nanoparticles are incorporated into the pancreas tumor, while OARs remain significantly unaffected. The gold nanoparticles present a DEF of 1.21, and barium titanate nanoparticles present a DEF of 1.14 at the tumor site. The increase in absorbed dose in the non-tumor pancreas was 4% in the presence of $BaTiO_3$ and 5% in the presence of gold nanoparticles. Also, the absorbed dose in OARs was increased by 0.5% to 3% in the presence of gold nanoparticles and by 0% to 2% for $BaTiO_3$ nanoparticles.

Figure 5 shows the microscopic and macroscopic DEF values. The results show that dose absorption is increased in the vicinity of clusters of both barium titanate and gold nanoparticles. Microscopic (lattice) values of 1.7 and 1.31 were calculated for barium titanate and gold nanoparticles, respectively. Also, microscopic DEF (sub-lattice) values of

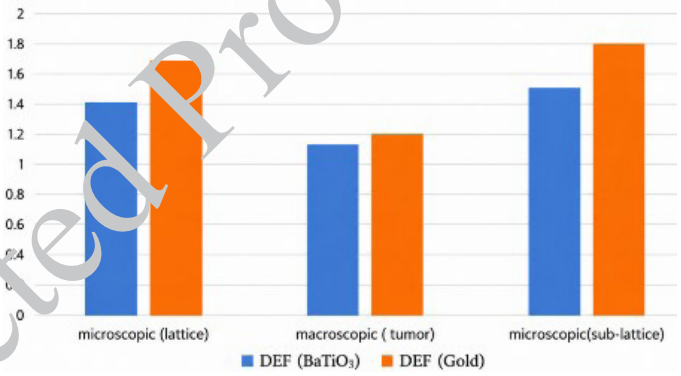

Figure 5. Comparison of macroscopic (pancreatic tumor) and microscopic (lattice and sub-lattice) DEF values for gold and $BaTiO_3$ nanoparticles in proton therapy
DEF: dose enhancement factor; $BaTiO_3$: Barium titanate

1.83 and 1.51 were calculated for barium titanate and gold nanoparticles, respectively.

Discussion

Based on the results, both gold and barium titanate nanoparticles have radiosensitization potential, with gold showing a higher dose enhancement effect than the $BaTiO_3$

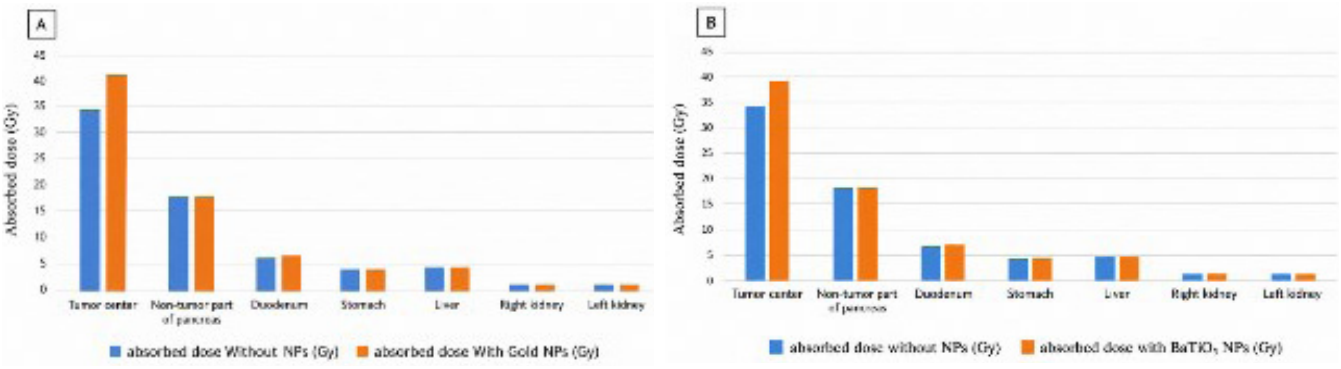

Figure 4. Macroscopic DEF values for the center of the tumor, the non-tumor part of the pancreas, and organs at risk
A) in the presence of gold nanoparticles. B) in the presence of barium titanate nanoparticles.
DEF: dose enhancement factor

Corrected Proof

nanoparticle (7%). Gold nanoparticles under proton beams amplify the local dose primarily through ionization and emission of proton-induced X-rays and Auger electrons resulting from Coulomb interactions between protons and extranuclear electrons of target atoms. The produced Auger electrons may further interact with electrons from adjacent atoms, leading to the generation of secondary electrons through multiple scattering events in the nanoscale vicinity of the nanoparticle. $BaTiO_3$ nanoparticles, although lower in atomic number than gold, still demonstrated a measurable dose enhancement. Their effect arises from a similar mechanism. The superior dose enhancement observed with gold nanoparticles compared to barium titanate under 135 MeV proton irradiation is primarily attributable to gold's high atomic number (Z=79 vs. Z_eff ≈ 38), which substantially increases stopping power and secondary electron production. Electronic interactions dominate energy deposition (~95% of total dose), with gold exhibiting ~60% higher mass stopping power than $BaTiO_3$ according to Bethe-Bloch theory (14, 15). Critically, Auger electron emission—scaling approximately as Z^4—is dramatically enhanced in high-Z materials, delivering a highly localized nanoscale dose particularly effective for inducing clustered DNA damage (16). Additionally, energetic delta-rays (secondary electrons) generated from ionization events propagate further in gold-loaded regions, extending dose deposition beyond the nanoparticle immediate vicinity (17). While nuclear fragmentation contributes <5% to total dose at therapeutic energies, the synergistic electronic mechanisms account for the observed superiority of gold nanoparticles in dose enhancement (18). Cho *et al.* (19) investigated the radioenhancement mechanisms of gold nanoparticles under proton beams. They found that particle-induced X-ray emission (PIXE) and particle-induced gamma-ray emission (PIGE) contribute less to dose deposition, while secondary electrons are the main contributors. Importantly, $BaTiO_3$ is well known for its excellent biocompatibility and low cytotoxicity in various biological models, making it a safer option for clinical translation compared to gold nanoparticles, which may elicit dose- and size-dependent toxicity and immunogenicity (8).

Several studies have confirmed the dose enhancement effect of metallic nanoparticles on proton therapy outcomes (3). Gold nanoparticles act as radiosensitizers by amplifying the generation of secondary electrons and reactive oxygen species upon proton irradiation. A study by Cunningham *et al.* (20) confirmed the radiosensitization potential of gold nanoparticles in proton therapy. A simulation study by Tabbakh *et al.* (21) reported the dose enhancement effect of gold nanoparticles in proton therapy. They found that the slowed-down protons by gold nanoparticles are the main contributors to the obtained extra dose. In contrast, the secondary electrons emitted from the gold nanoparticles contribute one order lower. Ceramic nanoparticles were studied as radiosensitizers in proton therapy. A Monte Carlo study by Ganjeh *et al.* (22) demonstrated the radioenhncement potential of Ta_2O_5 as a ceramic material in proton therapy. In a simulation study by McKinnon *et al.* (23), the radiosensitization potential of ceramic nanoparticles of Ta_2O_5 and CeO_2 in proton therapy was evaluated. The results showed a 14% to 17% enhancement in energy deposition for protons of 5 to 50 MeV. Engels *et al.* (24) conducted a Monte Carlo study based on experimental findings and showed that the nanoparticle shell of Ta2O5 induced highly localized physical dose enhancements during radiotherapy.

Based on the results, microscopic DEF values are higher than macroscopic physical DEF values in the tumor, confirming that proton-irradiated nanoparticles deposit their energy in proximity to themselves. The 10–20% macroscopic dose enhancement means that with the same exposed radiation, the delivered dose is increased 10-20% in the tumor. Clinically, this could allow for lower physical proton doses to achieve equivalent or superior tumor control, potentially widening the therapeutic window beyond reduction of OAR dose and side effects of proton therapy. High-Z nanoparticles exhibit substantially increased interaction cross-sections with incident protons, generating cascades of low-energy secondary electrons with short ranges (≤10 μm) that deposit energy in highly localized regions around the nanoparticle surface. Additionally, protons undergo intensive Coulomb scattering near nanoparticle interfaces, creating non-uniform dose distributions with localized hotspots that remain undetectable at macroscopic scales. At microscopic dimensions, the breakdown of charged particle equilibrium occurs because secondary electron ranges become comparable to the region of interest. Furthermore, nuclear interactions and atomic relaxation processes in High-Z materials generate Auger electron cascades with nanoscopic ranges that deposit energy exclusively in the immediate nanoparticle vicinity. In alignment with our study, a Monte Carlo study by Wälzlein *et al.* (6) showed that the physical dose enhancement effect of platinum nanoparticles under proton beams is the result of Auger cascades and secondary electron production, which is confined to a localized dose enhancement in a short range of a few nanometers from the nanoparticle. A Simulation study by Lin *et al.* (15) indicated that proton therapy can be enhanced significantly only if the gold nanoparticles are in proximity to the biological target. Cho *et al.* (19) found that proton-induced dose enhancement is up to 17 in the close vicinity (<100 nm) of gold nanorods, while the dose enhancement was about 1% in the whole of the simulated vial. They also found that particle-induced X-ray emission (PIXE) and particle-induced gamma-ray emission (PIGE) contribute less to dose deposition, while Auger electrons are the main contributors. Kwon *et al.* (25) simulated a single gold nanoparticle within water exposed to a proton beam and calculated the radial dose distribution due to secondary electrons. They found that the dose distribution due to the presence of gold nanoparticles is extended over several nanometers in the radial direction. Lin *et al.* (26) studied the enhancement mechanisms of proton beams in the presence of gold nanoparticles. They found that the highest enhancement for proton beams is closer to the nanoparticles (DEF=2 to 3 close to the nanoparticle and ~1.4 at a far distance).

The results of this study confirm the fact that both gold and barium titanate radioenhancement mainly remains localized to the tumor site. This selective enhancement improves the therapeutic index, increasing tumor dose without exceeding tolerances for surrounding healthy tissue. Proton beams with different interaction mechanisms produce dense ionization with high LET localized at the tumor region, providing a highly conformal dose distribution (27). Nanoparticles enhance proton therapy outcomes by amplifying the production of delta electrons and Auger electrons, which have a high LET (linear energy

Corrected Proof

transfer) with an extremely short range, typically on the order of nanometers (28). These electrons are responsible for enhanced local dose deposition at the nanoscale, increasing the likelihood of DNA damage within tumor cells and boosting cancer cell destruction, particularly in the Bragg Peak region. A key finding of this study is the preferential enhancement of dose within the tumor volume, with minimal impact on surrounding healthy pancreatic tissue and OARs. In a simulation study using the MCNP6 code, Rahmawat *et al.* (29) simulated the lung with a 3 cm tumor surrounded by OARs irradiated by proton beams. Their results show that OARs are safe in proton therapy.

Several nanoparticles, such as hafnium oxide and gadolinium-based ones, have advanced to clinical trials (5). In an *in vivo* study by Filimonova *et al.* (30), they showed that bismuth nanoparticles injected directly into the tumor enhanced the antitumor effects of proton therapy. An *in vitro* study by Liu *et al.* (31) confirmed the radiosensitization effect of gold nanoparticles in proton therapy, evidenced by a considerable reduction in the survival fraction of EMT-6 and CT26 cell lines. Kim *et al.* (32) investigated the radioenhancement effect of gold and iron nanoparticles in proton therapy with a 40 MeV therapeutic proton beam. They reported a 37% to 62% increase in complete CT26 tumor regression in mice when the Bragg peak was located in the tumor center. An experimental study on prostate tumor cells exposed to 160 MeV protons demonstrated a 15% to 20% increase in prostate tumor cell killing when gold nanoparticles were applied (33). $BaTiO_3$ is a ferroelectric ceramic, meaning it has internal electric fields that may influence biological systems at the nanoscale, leading to the generation of oxidative stress and apoptosis in cancer cells. Although the mechanism of therapeutic enhancement of nanoparticles in proton therapy is still under discussion, investigations based on proton radiobiology show a proton beam-induced generation of nanoradiators and reactive oxygen species (ROS) and their subsequent action on cancer cells, leading to DNA damage and apoptosis (34). Babychamy *et al.* (35) found that oxidant and antioxidant levels in cells can be altered by proton irradiation. Titanium dioxide is known as a low-Z metal oxide nanomaterial characterized by a high surface-to-volume ratio and a notable biological inertness (36). Gerken *et al.* (37) showed that irradiation of titanium dioxide by proton beams leads to the generation of a significant amount of ROS and 290% radioenhncement. The nuclear reaction that occurs when titanium interacts with protons, specifically through the reaction 48Ti (p, x) 48V, results in the formation of the radioactive isotope 48V, which emits positrons (38). This phenomenon may be linked to the markedly enhanced radiobiological effects of titanium dioxide under proton irradiation. Ahamed *et al.* (39) demonstrated that $BaTiO_3$ nanoparticles could significantly elevate reactive oxygen species (ROS) production, cause DNA damage, and activate apoptosis pathways in lung carcinoma cells. Abdul Rashid *et al.* (27) studied the radiosensitization efficacy of gold, bismuth, iron oxide, and platinum nanoparticles on HCT116 colon carcinoma cells exposed to 150 MeV protons. Their results show that nanoparticles could enhance ROS production and dose deposition, leading to a reduction in cell viability. Also, their results indicate that bismuth has the highest ROS production ability, followed by gold, platinum, and iron oxide, respectively.

Study limitations and suggestions

In this study, the homogeneous nanoparticle distribution was assumed to provide a controlled framework for comparing gold and $BaTiO_3$ nanoparticles under identical conditions. However, nanoparticle uptake is heterogeneous *in vivo* and may result in localized variations in DEF. Future studies should incorporate more realistic nanoparticle distributions to provide a more comprehensive evaluation of dose enhancement.

This simulation study reveals the physical radiosensitization potential of barium titanate nanoparticles compared to gold nanoparticles, which limits the results of this study to the direct effects of the proton beam, not considering the indirect effects. Notably, ROS production is normally found to correlate with the level of radiosensitization and plays an essential role in the radiosensitization mechanisms; further simulation and experimental studies are needed on the physicochemical dose enhancement (ROS production) and biological radioenhancement effects of $BaTiO_3$ nanoparticles under proton irradiation.

Conclusion

This nanolattice-based simulation framework provides a novel approach to modeling nanoparticle distributions within tumors. In this study, the physical dose enhancement potential of barium titanate and gold nanoparticles loaded in a pancreatic tumor under proton beam irradiation was investigated. Both gold and $BaTiO_3$ nanoparticles demonstrate promising macroscopic and microscopic DEF values, with gold nanoparticles showing a higher dose enhancement effect than barium titanate nanoparticles. Also, the results show that the microscopic dose enhancement value is higher than the macroscopic dose enhancement value, confirming that most proton-induced dose enhancement occurs in the close vicinity of nanoparticles. Further simulation studies on the physicochemical dose enhancement (ROS production) of $BaTiO_3$ nanoparticles and experimental studies are suggested.

Acknowledgment

This paper was supported by the Medical Radiation Sciences Research Center of Tabriz University of Medical Sciences (IR.TBZMED.VCR.REC.1403.279). We are grateful to the Tabriz University of Medical Science Research Vice-Chancellor for supporting this research.

Authors' Contributions

E M conceived the study, performed the simulations, analyzed the data, and prepared the original draft of the manuscript. P M supervised the study and contributed to the scientific and language editing of the manuscript. Both authors reviewed and approved the final version of the manuscript.

Conflicts of interest

The authors declare no conflict of interest

Declaration

We acknowledge the use of ChatGPT to enhance the figures quality.

References

1. Bazeed AY, Day CA-O, Garg SA-O. Pancreatic cancer: Challenges and opportunities in locoregional therapies. Cancers

Corrected Proof

(Basel) 2022;14:4257.
2. Kobeissi JA-O, Simone CBnA-O, Lin H, Hilal LA-O, Hajj C. Proton therapy in the management of pancreatic cancer. Cancers (Basel) 2022;14:2789.
3. Ma J, Shen H, Mi ZA-O. Enhancing proton therapy efficacy through nanoparticle-mediated radiosensitization. Cells 13:1841.
4. Mansouri E, Almisned G, Tekin HO, Rajabpour S, Mesbahi A. Radiosensitization with metallic nanoparticles under MeV proton beams: local dose enhancement. Radiat Environ Biophys 2024; 63:537-543.
5. Liu Y, Li B, Wang L. Potential applications of metal-based nanomaterials in tumor radiotherapy: from x-ray to particle therapies. Cancer Nanotechnol 2025; 16:42.
6. Ma J, Shen H, Mi Z. Enhancing proton therapy efficacy through nanoparticle-mediated radiosensitization. Cells 2024; 13:1841.
7. Montazersaheb S, Farahzadi R, Mansouri E, Jafari S, Fathi E. Radiosensitizing effects of silver nanoparticles targeting angiogenesis and matrix metalloproteinase signaling in triple negative breast cancer cell lines. Sci Rep 2026;16:6820.
8. Raj D, M.V M, K S, Mohan CC, Bhat SG. Anticancer potential of Barium titanate nanoparticles: Structural, optical and biomedical perspectives. Results Surf. Interfaces 2025; 20:100584.
9.Mansouri E, Mesbahi A, Hejazi MS, Tarhriz V, Hamishehkar H, Seyednejad F. A comprehensive analysis of radiosensitization properties of metallic nanoparticles in brachytherapy of gastric adenocarcinoma by I-125 seed: A simulation study by MCNPX and MCNP6 codes. Magnetochemistry 2022; 8:1-10.
10. Çağlar MA-O, Eşitmez DA-O, Cebe MA-O. The Effect of Dose Enhancement in Tumor With Silver Nanoparticles on Surrounding Healthy Tissues: A Monte Carlo Study. Technol Cancer Res Treat 2024; 23:15330338241235771.
11. Zhang X, Xie X, Qu D, Ning J, Zhou H, Pan J, *et al.* Determining organ dose conversion coefficients for external neutron irradiation by using a voxel mouse model. J Radiat Res 2016;57:182-188.
12. Hadiyan fard M, Baghani HR, Shamsabadi R, Aminafshar B. Effect of nanoparticle distribution scenario on tissue dose corrections: A Monte Carlo simulation study. Radiat Phys Chem 2026; 244:113806.
13. Martinov MP, Fletcher EM, Thomson RM. Multiscale monte Carlo simulations of gold nanoparticle dose-enhanced radiotherapy I: Cellular dose enhancement in microscopic models. Med Phys 2023;50:5842-5852.
14. Sung W, Ye SJ, McNamara AL, McMahon SJ, Hainfeld J, Shin J *et al.* Dependence of gold nanoparticle radiosensitization on cell geometry. Nanoscale 2017;9:5843-5853.
15. Lin Y, McMahon SJ, Scarpelli M, Paganetti H, Schuemann J. Comparing gold nano-particle enhanced radiotherapy with protons, megavoltage photons and kilovoltage photons: A Monte Carlo simulation. Comparative Study Phys Med Biol 2014;59:7675-7689.
16. Misawa M, Takahashi J. Generation of reactive oxygen species induced by gold nanoparticles under x-ray and UV Irradiations. Nanomed Nanotechnol Biol Med 2011; 7: 604-614.
17. McMahon SJ, Hyland WB, Muir MF, Coulter JA, Jain S, Butterworth KT, *et al.* Biological consequences of nanoscale energy deposition near irradiated heavy atom nanoparticles. Sci Rep 2011; 1:18.
18. Hainfeld JF, Smilowitz HM, O'Connor MJ, Dilmanian FA, Slatkin DN. Gold nanoparticle imaging and radiotherapy of brain tumors in mice. Nanomedicine 2013;8:1601-1609.
19. Cho J, Gonzalez-Lepera C, Manohar N, Kerr M, Krishnan S, Cho SH. Quantitative investigation of physical factors contributing to gold nanoparticle-mediated proton dose enhancement. Phys Med Biol 2016; 61:2562-2581.
20. Cunningham C, de Kock M, Engelbrecht M, Miles X, Slabbert J, Vandevoorde C. Radiosensitization effect of gold nanoparticles in proton therapy. Front Public Health 2021; 9:699822.
21. Tabbakh F. Significance of the proton energy loss mechanism to gold nanoparticles in proton therapy: A Geant4 simulation. Sci Rep 2024; 14:24978.
22. Ahmadi Ganjeh Z, Salehi Z. Monte Carlo study of nanoparticles effectiveness on the dose enhancement when irradiated by protons. AIP Advances 2023; 13: 0350181-0350186.
23. McKinnon S, Guatelli S, Incerti S, Ivanchenko V, Konstantinov K, Corde S, *et al.* Local dose enhancement of proton therapy by ceramic oxide nanoparticles investigated with Geant4 simulations. Physica Medica 2016; 32:1584-1593.
24. Engels E, Corde S, McKinnon S, Incerti S, Konstantinov K, Rosenfeld A, *et al.* Optimizing dose enhancement with Ta_2O_5 nanoparticles for synchrotron microbeam activated radiation therapy. Physica Medica 2016; 32:1852-1861.
25. Kwon J, Sutherland K, Hashimoto T, Date H. Dose Distribution of electrons from gold nanoparticles by proton beam irradiation. Int J Med Phys Clin Eng Radiat Oncol 2015; 04:49-53.
26. Lin Y, McMahon Sj, Paganetti H, Paganetti H, Schuemann J, Schuemann J. Biological modeling of gold nanoparticle enhanced radiotherapy for proton therapy. Phys Med Biol 2015;60:4149-4168.
27. Abdul Rashid R, Zainal Abidin S, Khairil Anuar MA, Tominaga T, Akasaka H, Sasaki R, *et al.* Radiosensitization effects and ROS generation by high Z metallic nanoparticles on human colon carcinoma cell (HCT116) irradiated under 150 MeV proton beam. OpenNano 2019; 4:100027.
28. Wälzlein C, Scifoni E, Krämer M, Durante M. Simulations of dose enhancement for heavy atom nanoparticles irradiated by protons. Phys Med Biol 2014; 59:1441.
29. Rahmawati F, Khairunnisa AF, Riyatun, Suharyana. Analysis of dose distribution in proton therapy for lung cancer with MCNP code. J Phys Conf 2022; 2190:012021.
30. Filimonova MV, Soldatova OV, Shitova AA, Filimonov AS, Rybachuk VA, Kosachenko AO, *et al.* Bismuth nanoparticles increase effectiveness of proton therapy of ehrlich carcinoma. Bull Exp Biol Med 2024; 176:626-630.
31. Liu C-J, Wang C-H, Chen S-T, Chen H-H, Leng W-H, Chien C-C, *et al.* Enhancement of cell radiation sensitivity by pegylated gold nanoparticles. Phys Med Biol 2010; 55:931.
32. Kim JK, Seo SJ, Kim KH, Kim TJ, Chung MH, Kim KR, Yang TK, *et al.* Therapeutic application of metallic nanoparticles combined with particle-induced x-ray emission effect. Nanotechnology 2010; 21:425102.
33. Polf JC, Bronk LF, Driessen WHP, Arap W, Pasqualini R, Gillin M. Enhanced relative biological effectiveness of proton radiotherapy in tumor cells with internalized gold nanoparticles. Appl Phys Lett 2011; 98:193702.
34. Zavestovskaya IN, Filimonova MV, Popov AL, Zelepukin IV, Shemyakov AE, Tikhonowski GV, *et al.* Bismuth nanoparticles-enhanced proton therapy: Concept and biological assessment. Materials Today Nano 2024; 27:100508.
35. Baluchamy S, Ravichandran P, Periyakaruppan A, Ramesh V, Hall JC, Zhang Y, *et al.* Induction of cell death through alteration of oxidants and antioxidants in lung epithelial cells exposed to high energy protons. J Biol Chem 2010; 285:24769-24774.
36. Tucci P, Porta G, Agostini M, Dinsdale D, Iavicoli I, Cain K, *et al.* Metabolic effects of TiO_2 nanoparticles, a common component of sunscreens and cosmetics, on human keratinocytes. Cell Death Dis 2013; 4:e549-e549.
37. Gerken LRH, Gogos A, Starsich FHL, David H, Gerdes ME, Schiefer H, *et al.* Catalytic activity imperative for nanoparticle dose enhancement in photon and proton therapy. Nat Commun 2022; 13:3248.
38. Sadeghi M, Ansari Z, Kakavand T. Targetry for 48 V production and the nuclear model calculation on the charge particle induced reaction on Ti target. J Radioanal Nucl Chem 2012; 293:7-12.
39. Ahamed M, Akhtar MJ, Khan MAM, Alhadlaq HA, Alshamsan A. Barium titanate ($batio_3$) nanoparticles exert cytotoxicity through oxidative stress in human lung carcinoma (a549) cells. Nanomaterials 2020; 10:2309.

Corrected Proof